Digital shape analysis with maximal segments

Jacques-Olivier Lachaud[1]

Laboratory of Mathematics (LAMA CNRS 5127)
University of Savoie, 73376 Le Bourget-du-Lac, FRANCE
jacques-olivier.lachaud@univ-savoie.fr

Abstract. We show in this paper how a digital shape can be efficiently analyzed through the maximal segments defined along its digital contour. They are efficiently computable. They can be used to prove the multigrid convergence of several geometric estimators. Their asymptotic properties can be used to estimate the local amount of noise along the shape, through a multiscale analysis.
Keywords discrete geometry; digital shape analysis; digital straight segments; geometric estimators; multigrid convergence; noise detection; digital convexity

1 Introduction

It is often interesting to study the geometry of digitization of Euclidean shapes in the plane, and to establish connections between the discrete geometry computed along the digital contour and the Euclidean geometry of the initial shape. This task is essential in image analysis, where the initial Euclidean shape has been lost through various acquisition and segmentation processes.

Maximal segments are the connected pieces of digital straight lines that are contained in the digital contour and that are not extensible [11, 12] (if they are extended on either side, the formed set is no more a digital straight segment). Maximal segments appear to hold many interesting properties for analyzing digital shapes. We will show here that they characterize the convex and concave parts of the shape [9, 11]. They induce discrete geometric estimators of length and tangent that are multigrid convergent, with a quantifiable error [20, 22]. These asymptotic properties of maximal segments [7] are also extremely useful to detect the local meaningful scales at which the shape should be analyzed: in this sense, they provide an unsupervised method to determine locally the level of noise that is damaging the shape [15].

2 Digital shapes, digital straightness, maximal segments and convexity

2.1 Digital shapes and shape digitization

A *digital shape* is a subset of the digital plane $\mathbb{Z}^2$. To simplify the exposition, this shape is simply connected (i.e. a polyomino). Its interpixel boundary is therefore

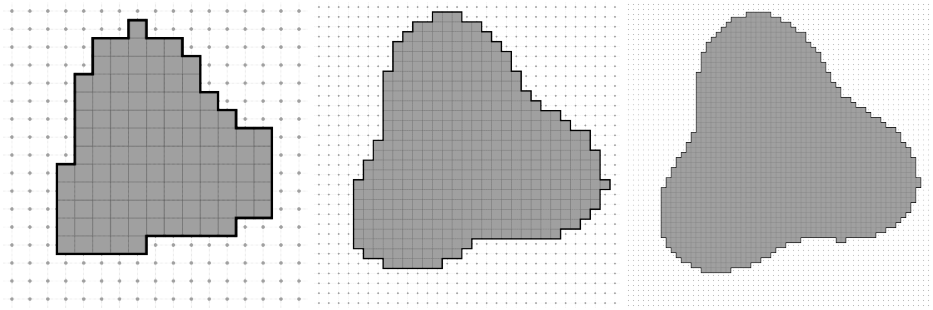

(a) $\mathrm{Dig}_1(X)$ (b) $\mathrm{Dig}_{\frac{1}{2}}(X)$ (c) $\mathrm{Dig}_{\frac{1}{4}}(X)$

Fig. 1. Euclidean shape digitized at finer and finer steps. The interpixel contour of the digitized shape forms a 4-connected path in some digital plane of half-integers.

a 4-connected contour in the half-integer plane. By translating everything by vector $(\frac{1}{2}, \frac{1}{2})$, we get back that all pointels of the interpixel boundary have integer coordinates. The so-formed 4-connected sequence of digital points is called the *digital contour* of the digital shape, and will be subsequently denoted by C. The integer N will stand for the number of points of this contour.

Digital shapes are obtained through the digitization process of Euclidean shapes. Let Dig_h be the Gauss digitization process of gridstep h, i.e., for any subset X of the plane $\mathbb{R}^2$, $\mathrm{Dig}_h(X) = X \cap (h\mathbb{Z} \times h\mathbb{Z})$. For a positive decreasing sequence of gridsteps (h_i), the family $(\mathrm{Dig}_{h_i}(X))$ is composed of digital shapes, which are finer and finer digital approximation of the Euclidean shape X (see Fig. 1). The contour of a digitized shape is not necessarily 4-connected since topological problems may occur. Gross and Latecki [13] and Latecki *et al.* [23] have studied the topological properties of digitized shapes for three digitization processes (intersection, subset, and area). They have shown that, for all these processes and for any simply connected par(r)-regular shape X, the contour of $\mathrm{Dig}_h(X)$ is a polyomino for $0 < h \leq r$. A similar property holds for the Gauss digitization process ([20], Theorem B.5, p. 149) but for $0 < h < \frac{\sqrt{10}}{5} r$.

Smooth Euclidean shapes with C^2-boundary and bounded curvature are par(r)-regular for some r. Therefore we will focus on digital shapes which are digitizations of par(r)-regular shapes and which are digitized with a sufficiently small gridstep. All considered digital contours will thus be polyominos.

2.2 Digital straightness

A *standard digital straight line (DSL)* is a 4-connected digital set $\{(x, y) \in \mathbb{Z}^2, \mu \leq ax - by < \mu + |a| + |b|\}$, all parameters being integers, with $\gcd(a, b) = 1$ [25]. Geometrically, the fraction a/b represents the slope of the line while parameter μ quantifies its shift at the origin. A *Digital Straight Segment (DSS)* is a finite 4-connected piece of DSL. Any DSS is included in an infinite number of DSL, but the *characteristics of the DSS* are the characteristics of the DSL

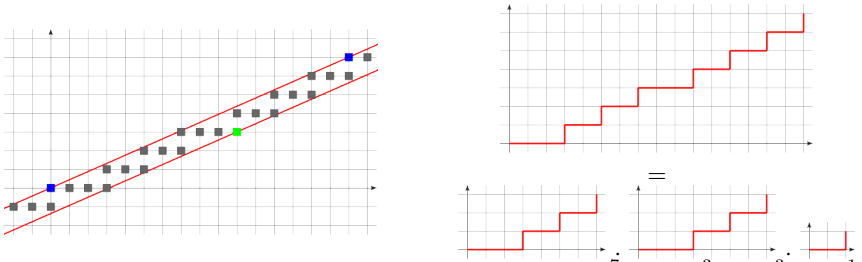

(a) DSL (7,16,0) (b) pattern $E(\frac{7}{16}) = E(\frac{3}{7}) \cdot E(\frac{3}{7}) \cdot E(\frac{1}{2})$

Fig. 2. Two views of digital straightness. (a) Geometric view: the DSL has slope 7/16. Upper leaning points are in blue while lower leaning points are in red. (b) Combinatoric view: the path between two upper leaning points (or *pattern*) has a recursive definition and can be obtained by concatenation of simpler patterns.

containing it with minimal $|a|$. A DSS is uniquely determined from its characteristics and the starting and ending points. The *remainder* of a DSS — or a DSL — of characteristics (a, b, μ) is the function $(x, y) \mapsto ax - by$. *Upper leaning points* have remainder μ. *Lower leaning points* have remainder $\mu + |a| + |b| - 1$. It is easy to see that the convex hull of these points forms a strip in the plane of slope a/b which contains all points of the DSL. A geometric view of a digital straight line of slope $\frac{7}{16}$ is given on Fig. 2a.

Digital straightness has been studied a lot in the 90s (e.g. see Klette and Rosenfeld review [18] or [19]). We briefly present another vision of digital straightness which is combinatoric and related to continued fractions.

Given a standard line (a, b, μ), we call *pattern* of characteristics (a, b) the succession of Freeman moves between any two consecutive upper leaning points. The sequence of Freeman moves defined between any two consecutive lower leaning points is the previous word read from back to front and is called the *reversed pattern* (see [5, 7]). We say that a DSS is *primitive* whenever it contains one pattern of its slope or one reversed pattern of its slope (but not one of each).

As noted by several authors ([2,29], or the work of Berstel reported in [5,7]), the pattern of any slope can be constructed from the continued fraction of the slope. We recall that a *simple continued fraction* is an expression:

$$z = \frac{a}{b} = [u_0; u_1, \ldots, u_{n-1}, u_n] = u_0 + \cfrac{1}{u_1 + \cfrac{1}{\ldots + \cfrac{1}{u_{n-1} + \cfrac{1}{u_n}}}},$$

where n is the *depth* of the fraction, and u_0, u_1, etc, are all integers and called the *partial quotients*. We call *k-th convergent* the simple continued fraction formed of the k first partial quotients: $z_k = \frac{p_k}{q_k} = [u_0; u_1, \ldots, u_k]$. The function E takes a continued fraction z as input to build recursively the pattern of a DSS of slope z in the first quadrant.

$$E(z_{-2}) = 0, E(z_{-1}) = 1, \quad \text{and}, \forall i \geq 0, \quad \begin{cases} E(z_{2i+1}) = E(z_{2i})^{u_{2i+1}} E(z_{2i-1}), \\ E(z_{2i}) = E(z_{2i-2}) E(z_{2i-1})^{u_{2i}}. \end{cases}$$

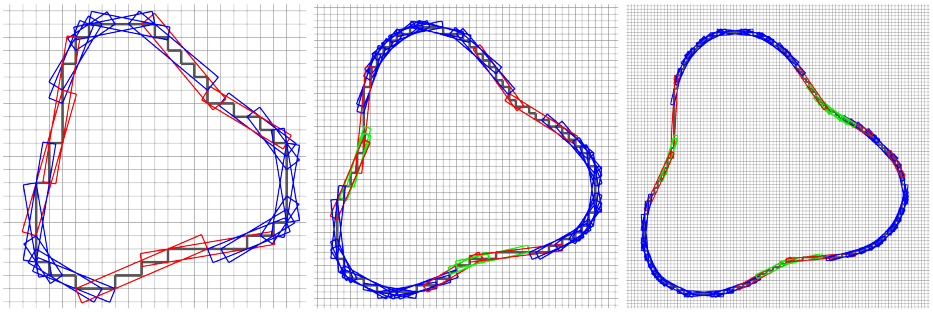

Fig. 3. Tangential cover of the flower shape of Fig. 1 for finer and finer gridsteps.

Let us take for example the fraction $\frac{7}{16} = [0; 2, 3, 2]$. The pattern of a DSL with this slope is thus (see Fig. 2(b) for an illustration) :

$$\begin{aligned} E([0;2,3,2]) &= E([0;2,3])^2 \cdot E([0;2]) & 00010010010001001001 \cdot 001 \\ E([0;2,3]) &= E([0]) \cdot E([0;2])^3 & 0 \cdot 001001001 \\ E([0;2]) &= 001 & 001 \\ E([0]) &= 0 & 0 \end{aligned}$$

Odd patterns (resp. *even* patterns) are patterns whose slope is a continued fraction with odd depth n (resp. even depth n). Patterns will be useful to establish the link between maximal segments and edges of convex digital shapes.

2.3 Maximal segments over a contour

If we consider the 4-connected path C, a *maximal segment* M is a subset of C that is a DSS and which is no more a DSS when adding any other points of $C \backslash M$. Fig. 4(a,b) displays the set of all the maximal segments covering the dark pixels. The sequence of all maximal segments along a digital contour is called the *tangential cover* [12]. The tangential cover of the "flower" shape is displayed on Fig. 3. As one can see, maximal segments look like local affine approximation of the shape boundary. We will show later in the paper that this is indeed true for several family of shapes.

It is worthy to note that the whole tangential cover of C can be computed in $O(N)$ time complexity. Indeed, online recognition of DSS takes $O(1)$ time complexity when adding a point [8], while updating the DSS characteristics when removing a point takes also $O(1)$ [12, 22]. Note that in the 90s, Smeulders and Dorst also proposed an algorithm to compute the tangential cover [28]. However, since it is based on repetitions (the relation with continued fractions was not used), it is much harder to understand and implement.

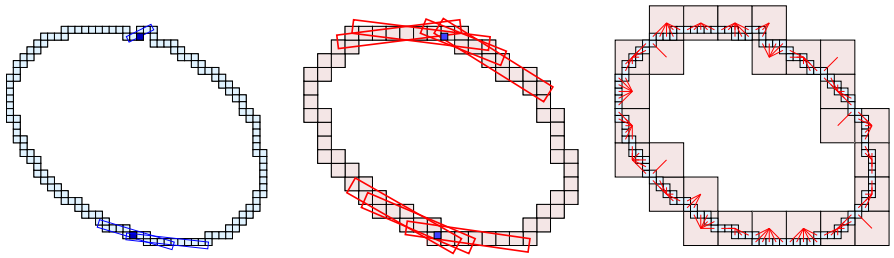

(a) (b) (c)

Fig. 4. Maximal segments on (a) an initial contour C and (b) on its subsampled contour $\phi_3^{0,0}(C)$. (c) Function $f_5^{0,0}$ (represented by lines) associating each pixel of C to its pixel of $\phi_5^{0,0}(C)$.

2.4 Maximal segments and convexity

Maximal segments are characteristics of the global convexity, but also give insights to the local convexity or concavity of the contour (illustrated on Fig. 5. More precisely:

A digital shape O (a subset of $\mathbb{Z}^2$) is *digitally convex* iff it is 4-connected and the Gauss digitization of the convex hull of O is O itself ($\text{Conv}(O) \cap \mathbb{Z}^2 = O$). By extension the contour of O is then said to be *digitally convex*.

Theorem 1 ([9]). *The contour of a polyomino is digitally convex if and only if the directions of its maximal segments are monotonous.*

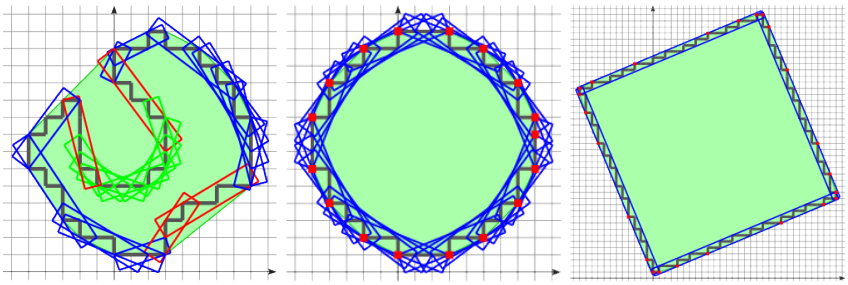

(a) (b) $n_{MS} = 24, n_e = 16$ (c) $n_{MS} = 4, n_e = 24$

Fig. 5. (a) Maximal segments and convexity. (b) and (c) number of maximal segments wrt number of edges of convex hull.

Inflexion maximal segments are maximal segments where slope directions are increasing on one side and decreasing on the other. They cut the contour of a digital shape into convex and concave parts. We will thus study the geometry of digital shapes by parts. Within each part, the contour will be digitally convex

(when concave, it suffices to inverse the role of foreground and background). We may therefore restrict our study to digitization of convex shapes, and most properties demonstrated on these shapes will remain valid for shapes with a finite number of inflexion points.

2.5 Maximal segments along digitally convex contours

If C is digitally convex, then the convex hull of its points forms a convex polygon $P(C)$ whose vertices have integer coordinates and are pointels of C (see red vertices in Fig. 5(b)). Edges of $P(C)$ thus partition C. Each part of C is called a *digital edge*. It is obvious that digital edges are DSS. More precisely, we have:

Proposition 1 ([7], Proposition 3.1). *Each digital edge of $P(C)$ is a pattern or a repetition of the same pattern.*

This implies that upper leaning points of maximal segments of C are to be found within the vertices of $P(C)$. A primitive DSS containing only a reversed pattern (thus no pattern) is called *LUL*. If not LUL, a DSS is called *ULU*. Maximal segments may thus be ULU or LUL. We can precisely relate maximal segments to digital edges with the following properties. All proofs combine geometric properties and pattern representation of DSS.

Lemma 1 ([7], Lemma 3.5). *Each ULU maximal segment of C contains a digital edge of $C(P)$ with exactly the same slope (which is called its* supporting edge*).*

Any LUL maximal segment of C has its upper leaning point that is a vertex of $C(P)$. This vertex is called its *supporting vertex*.

Lemma 2 ([7], Proposition 3.9 and 3.10). *Any vertex of $C(P)$ is the supporting vertex of at most one LUL maximal segment with even depth and of at most one LUL maximal segment with odd depth.*

We denote by $n_{MS}(C)$ the number of maximal segments of C and $n_e(P(C))$ the number of edges of $P(C)$. As shown on Fig. 5(bc), the relation between n_e and n_{MS} was not clear. However Lemma 1 and Lemma 2 entails that $n_{MS}(C) \leq 3n_e(P(C))$.

Patterns are also used to obtain a lower bound on $n_{MS}(C)$ as a function of $n_e(P(C))$.

Lemma 3 ([7], Theorem 3.13). *An ULU maximal segment of slope z_n, $n \geq 2$, includes at most $2n+1$ edges (n on each side of the central pattern). A LUL maximal segment of slope z_n, $n \geq 2$, includes at most $2n$ edges.*

Figure 6 illustrates the origin of this result. Well-chosen subpatterns do not change the slope of a DSS but creates digital edges. By examining the constructive proof of the preceding lemma, we may deduce that the shortest maximal segment which includes $2n+1$ edges has a slope of the form $z_n = [0; 2, 2, \ldots, 2]$.

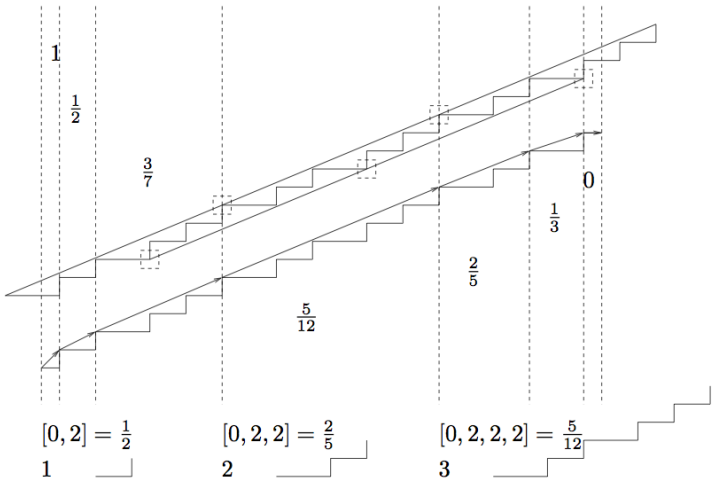

Fig. 6. Shortest maximal segment which contains the greatest number of digital edges: DSS with slope $[0; 2, 2, \ldots, 2]$. For instance, the edges to the left are $0^{u_1-1}1$, ..., $E(z_{n-2})^{u_{n-1}-1}$, $E(z_{n-1})^{u_n-1}E(z_{n-2})$.

Since pattern length grows exponentially with its depth, a pattern included in a $m \times m$ grid has a depth upper bounded by $\theta(\log(m))$.

Since maximal segments cover the contour, it is then clear that $n_{MS}(C) \geq \frac{n_e(P(C))}{\theta(\log(m))}$, where $m \times m$ is the bounded box of C.

Putting everything together, we may conclude the following result for digitizations of sufficiently smooth convex shapes:

Theorem 2 ([7], Theorem 3.15). *For a finite convex shape X, let C_h be the digital boundary of* $\mathrm{Dig}_h(X)$*. We have*

$$\frac{n_e(P(C_h))}{\alpha_1(\log \frac{1}{h}) + \alpha_2} \leq n_{MS}(C_h) \leq 3n_e(P(C_h)).$$

with $\alpha_1 \approx 2.269$, $\alpha_2 \approx 1.359$.

Other results relating the length of maximal segments with the length of digital edges can be found in the same reference.

Proposition 2 ([7], Proposition 4.1 and 4.2, with [5], Proposition 3.1.5). *The digital lengths of an ULU maximal segment and its supporting edge are linearly related. The same holds for a LUL maximal segment with one of the edge around its supporting vertex.*

We conclude this section with another interesting result on maximal segments that indicates how many maximal segments cover a point on a contour. This

result was not obvious since Feschet [11] has exhibited a way to construct a contour such that, for any integer k, there is a point on this shape with k maximal segments covering it.

Lemma 4 ([5], Proposition 3.2.13). *Given some contour C, the average number of maximal segments covering a point of C is upper bounded by 22.*

Figure 3(a,b,c) also indicates that the maximal segment are geometrically close to the tangents along the shape boundary. This remark will help us in designing multigrid convergent estimators.

3 Multigrid convergence and asymptotic properties

Multigrid convergence is an interesting way of relating digital and Euclidean geometries. The idea is to ask for discrete geometric estimations to converge toward the corresponding Euclidean quantity when considering finer and finer shape digitizations (here, Gauss digitization). Maximal segments allow the construction of multigrid convergent estimators of global geometric quantities (like length) and local geometric quantities (tangent).

3.1 Multigrid convergence for global geometric quantities

Definition 1 (Definition 2.10 of [19]). *A discrete geometric estimator $\hat{\mathcal{Q}}$ is* multigrid convergent *for a family of shapes $\mathcal{F}$ and a digitization process* Dig. *iff for all shape $X \in \mathcal{F}$, there exists a grid step $h_X > 0$ such that the estimate $\hat{\mathcal{Q}}(\mathrm{Dig}_h(X))$ is defined for all $0 < h < h_X$ and*

$$|\hat{\mathcal{Q}}(\mathrm{Dig}_h(X)) - \mathcal{Q}(X)| \leq \tau(h),$$

where $\tau : \mathbb{R}^+ \to \mathbb{R}^+$ with null limit at 0. This function is the speed of convergence *of the estimator.*

For instance, when $\mathcal{Q}$ is the area A of the shape, the estimator $\hat{A}(O) = h^2\mathrm{Card}(O)$ is multigrid convergent for most family of shapes (Gauss, Dirichlet as reported in [19], see also [14] for best known upper bound). Multigrid convergence has also been established for several length estimators (reported in [4]). The *minimum perimeter polygon* of a digital shape is multigrid convergent with speed $O(h)$ [27].

The minimum perimeter polygon of a digital contour C can be computed in optimal time $O(N)$ from its maximal segments [21, 24], and see also [26] for a very close approach. Therefore, maximal segments are useful to estimate the length of digitized shapes.

3.2 Multigrid convergence for local geometric quantities

Tangent direction, normal vector, curvature are local geometric quantities along the shape boundary. Each of them is thus some function of the shape boundary. However, the contour of the shape digitization does not define the same domain. Therefore we cannot directly compare the true geometric function with the estimated geometric function. We provide below a definition of multigrid convergence for discrete local estimators. It is neither a parametric definition as in [10] nor a point-wise definition as the standard multigrid convergence reported in [19]. Furthermore, for the sake of simplicity, there is no direct mapping between the contour and its digitized counterpart as proposed in [20]. It is a geometric definition, stating that any digital point sufficiently close to the point of interest has its estimated geometric quantity which tends toward the expected local value of the geometric function. This definition of multigrid convergence imposes shapes with continuous geometric fields. Of course, one can afterwards relax this constraint by splitting the shape boundary into individual parts where the geometric function is continuous.

Given a shape X in $\mathcal{F}$, and some x in the topological boundary ∂X of X, let $Q(X, x)$ be some local geometric quantity of ∂X at x. A *discrete local estimator* $\hat{Q}$ is a mapping which associates to any digital contour C, a point $y \in C$ and a gridstep h, some value in a vector space (e.g., $\mathbb{R}$ for the curvature). We are now in position to define the multigrid-convergence of this estimator:

Definition 2. *The estimator $\hat{Q}$ is* multigrid-convergent *for the family $\mathcal{F}$ if and only if, for any $X \in \mathcal{F}$, there exists a grid step $h_X > 0$ such that the estimate $\hat{Q}(\mathrm{Dig}_h(X), y, h)$ is defined for all $y \in \partial\mathrm{Dig}_h(X)$ with $0 < h < h_X$, and for any $x \in \partial X$,*

$$\forall y \in \partial\mathrm{Dig}_h(X) \text{ with } \|y - x\|_1 \leq h, |\hat{Q}(\mathrm{Dig}_h(X), y, h) - Q(X, x)| \leq \tau_{X,x}(h),$$

where $\tau_{X,x} : \mathbb{R}^{+*} \to \mathbb{R}^+$ has null limit at 0. This function defines the speed of convergence of $\hat{Q}$ toward Q at point x of ∂X. The convergence is uniform *for X when every $\tau_{X,x}$ is bounded from above by a function τ_X independent of $x \in \partial X$ with null limit at 0.*

It is worth noting that, for sufficiently regular shapes (par(r)-regular shapes [23]), there exists a gridstep below which the boundary of the shape digitization has same topology as the shape boundary ([20], Theorem B.5). Furthermore, these two boundaries are very close. Indeed, there exists a gridstep below which for any $x \in X$ there is a $y \in \partial\mathrm{Dig}_h(X)$ with $\|y - x\|_1 \leq h$ and conversely for any $y \in \partial\mathrm{Dig}_h(X)$, there is a $x \in X$ with $\|y - x\|_1 \leq h$ ([20], Lemma B.9). Therefore the previous definition of multigrid convergence guarantees that the estimated local quantity converges toward the true local geometric quantity everywhere along the shape boundary.

3.3 Convergent tangent estimation with maximal segments

As observed in [3] and stated in [7, 22], the slope of maximal segments tend to approximate the slope of the tangent of the underlying points. This result

is achieved by establishing some asymptotic properties of maximal segments along a digitized shape as the digitization step tends to 0. To get the behavior of the average length of maximal segments, we combine the behavior of the number of maximal segments (Theorem 2) with the properties on their length (Proposition 2), which gives:

Theorem 3 ([7], Theorem 4.4). *For a finite convex shape X, let C_h be the digital boundary of $\mathrm{Dig}_h(X)$, and $(MS_i)_{i=1..n_{MS}(C_h)}$ be its maximal segments. The following inequalities hold*

$$\frac{1}{3}\frac{\mathrm{Per}(P(C_h))}{n_e(P(C_h))} \leq \frac{\sum_{i=1}^{n_{MS}(C_h)} \mathcal{L}^1(MS_i)}{n_{MS}(C_h)} \leq \Theta(\log\frac{1}{h})\frac{\mathrm{Per}(P(C_h))}{n_e(P(C_h))}.$$

The average digital length of maximal segments is almost proportionnal to the average digital length of digital edges. Now, Theorem 2 of Balog et Bárány [1] indicates that the average digital length of digital edges of digitization of shapes X with C^3-boundary and strictly positive curvature is some $\Theta(h^{-\frac{1}{3}})$. By relating this result to Theorem 3, we obtain:

Theorem 4 (Theorem 5.1 of [7] and Theorem 5.26 of [20])). *With X and C_h defined as above, digital lengths of maximal segments follow:*

$$\textit{average } \overline{L}_{MS}\textit{:} \quad \Theta(h^{-\frac{1}{3}}) \leq \overline{L}_{MS}(C_h) \leq \Theta(h^{-\frac{1}{3}}\log\frac{1}{h}) \tag{1}$$

$$\textit{shortest } L^{\min}_{MS}\textit{:} \quad \Theta(h^{-\frac{1}{3}}) \leq L^{\min}_{MS}(C_h) \tag{2}$$

$$\textit{longest } L^{\max}_{MS}\textit{:} \quad L^{\max}_{MS}(C_h) \leq \Theta(h^{-\frac{1}{2}}) \tag{3}$$

As one can see, the digital length of maximal segments grows as the resolution gets finer. Therefore, estimating the tangent direction at some point as the direction of any maximal segment covering it leads to a discrete tangent estimator that is uniformly convergent in $O(h^{\frac{1}{3}})$ (from (2) and Taylor expansion [20,22]). More precisely, this property of maximal segments induces that for any point $P \in C$:

1. the tangent at P estimated by the most centered maximal segment covering P (estimator of [12]),
2. the tangent at P estimated as a convex combination of maximal segments covering P (λ-MST estimator of [22]),
3. the tangent at P estimated as derivative of Gaussian of kernel size equal to a maximal segment covering P (Hybrid Gaussian Derivative estimator of [6]),

are uniformly multigrid convergent with speed $\Theta(h^{\frac{1}{3}})$. Their convergence speed is experimentally $O(h^{\frac{2}{3}})$ nearly everywhere.

Furthermore, the length of any digital path can be estimated by integrating at each linel the scalar product of its tangent estimation and the linel direction. The preceding result induces a multigrid convergent length estimator with speed $O(h^{\frac{1}{3}})$. It is also interesting to notice that (1) refutes the hypothesis used in the proof of the multigrid convergence of the curvature estimator by circumscribed circle (Theorem B.4, [3]). This estimator is also not convergent experimentally.

4 Reverse asymptotic, meaningful scales and noise detection

The preceding asymptotic properties can be used to detect the meaningful scales at which a shape should be locally considered [15,17]. Indeed, let x be some point on ∂X. We denote by (L_j^h) the discrete lengths of the maximal segments, defined along $\partial \mathrm{Dig}_h(X)$, and which cover x. If U is an open connected neighborhood of x on X, Theorem 4 induces (4) (Equation (5) is rather straightforward):

$$\text{if } U \text{ is strictly convex or concave, then } \Omega(1/h^{1/3}) \leq L_j^h \leq O(1/h^{1/2}) \quad (4)$$

$$\text{if } U \text{ has null curvature everywhere, then } \Omega(1/h) \leq L_j^h \leq O(1/h). \quad (5)$$

In practice, we only have a digital shape O as input data at some scale. It is thus not possible to obtain the asymptotic digitizations of the original shape X with finer and finer grid steps h. A solution is to observe the asymptotic but in the reverse direction, i.e. with coarser and coarser grid steps. We then consider the subsampling $\phi_i^{x_0,y_0}(O)$ with increasing covering pixel sizes $i \times i$ for $i = 2, .., n$ and with shift x_0, y_0. Several subsampling processes can be considered at this stage, but it is necessary to maintain a surjective map $f_i^{x_0,y_0}$ which associates any point P of C to its image point in the subsampled contour $\phi_i^{x_0,y_0}(C)$. Such a function is illustrated on Fig. 4(c). Then, we can consider the discrete lengths $(L_j^{h_i,x_0,y_0})$ of the maximal segments on the subsampled shapes $\phi_i^{x_0,y_0}(C)$ containing $f_i^{x_0,y_0}(P)$ with the increasing sequence of digitization grid steps $h_i = ih$ (see Fig. 4(a,b)). For a given subsampling size i, the average digital length of all the maximal segments containing the subsampled pixel is denoted as $\overline{L}^{h_i}$.

The *multiscale profile* $\mathcal{P}_n(P)$ at point P is defined as the sequence of samples $(X_i, Y_i) = (log(i), log(\overline{L}^{h_i}))_{i=1..n}$ (see Fig. 7(a,b)). According to (4) (resp. (5)), if P is located on a curved (resp. flat) part, the slope of an affine approximation of the multiscale profile should be in $[-\frac{1}{2}, -\frac{1}{3}]$ (resp. $[-1, -\frac{1}{2}]$). Since for noisy contour parts the preceding properties are not valid, an invalid slope detects them directly. A threshold t_m is given to determine the *meaningful scale* defined as a pair (i_1, i_2), $1 \leq i_1 < i_2 \leq n$, such that for all i, $i_1 \leq i < i_2$, $\frac{Y_{i+1}-Y_i}{X_{i+1}-X_i} \leq t_m$. For the example of Fig. 7, the meaningful scales of the points P_1 and P_2 are respectively equal to $(1, 15)$ and $(3, 15)$.

The *noise level* $\nu(P)$ of a point P is the integer $i_1 - 1$, where (i_1, i_2) is the first meaningful scale at P. Experimentally the threshold value $t_m = 0$ gives best results both on curved or flat noisy parts. Figure 8 shows some results obtained on various shapes. The noise detection appears to be well linked to the amount of noise, and is accurate and fast to compute.

Figure 9, left, gives another example of noise detection on the contour of a thresholded photography. Furthermore we can just threshold the slope of the meaningful scale to decide whether it is a curved part (slope is in $[-\frac{1}{2}, -\frac{1}{3}]$) or a flat part (slope is in $[-1, -\frac{1}{2}]$). The output of this simple classifier is displayed on Fig. 9, right.

The presented noise detector is available online at [16].

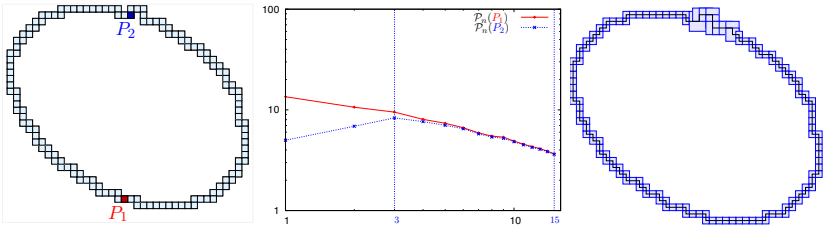

(a) (b) (c)

Fig. 7. Illustration of multiscale profile (b) on several points of the contour (a). (c) shows the resulting noise level estimation represented by a centered box of size $\nu(P)+1$.

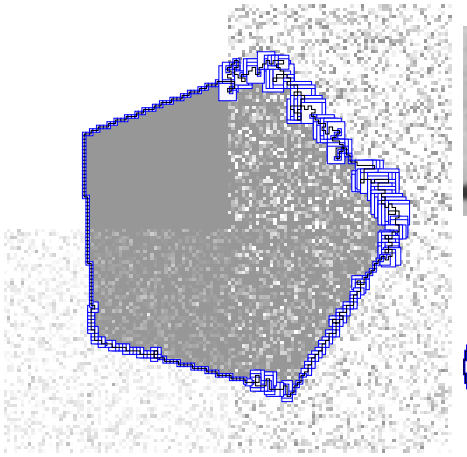

(a) 544 points, 293 ms

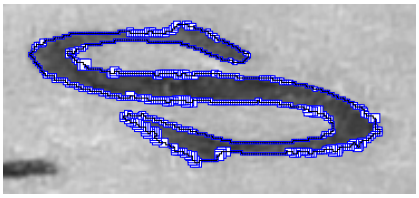

(b) 874 points, 445 ms

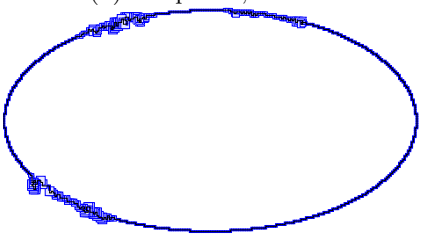

(c) 828 points, 430 ms

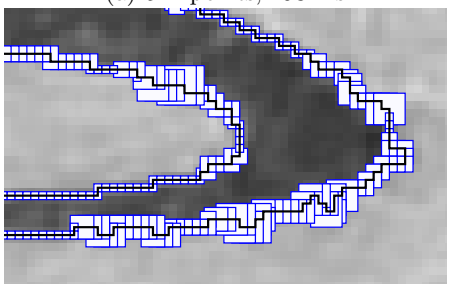

(d) zoom on lower-right of (b)

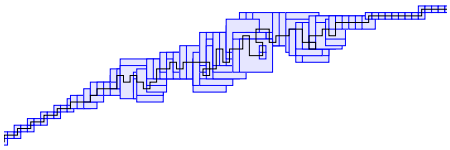

(e) zoom on upper-left part of (c).

Fig. 8. Noise detection obtained on various shapes (noise level locally represented by a centered box of size $\nu(P)+1$). The contour in (a) is a thresholding of the background image (Gaussian noise of variances $\sigma = 0, 50, 100, 150$ added by quadrant). (b) and (d): Experiments on a photography of a letter. (c) and (e): Noise detection on a synthetic object with noise added locally to the curve. Timings obtained on an *Intel Pentium 4, 3GHz, 1Go* with a maximal scale n equal to 15.

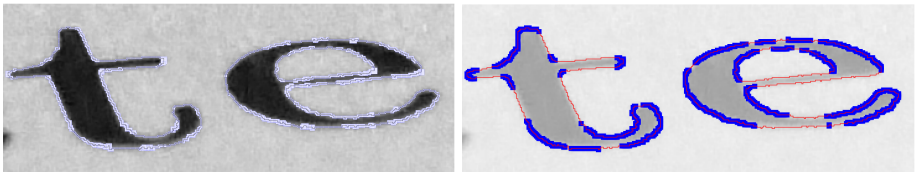

Fig. 9. Noise detection (left) and curve/flat zone classification (right) on real photography. The local noise level is represented by a box of corresponding size. Automatically classified curve parts are underlined in blue.

Further details on maximal segments and their applications can be found in [7, 15, 17, 20–22, 24].

References

1. A. Balog and I. Bárány. On the convex hull of the integer points in a disc. In *Proc. 7th Symp. on Computational geometry (SCG'91)*, pages 162–165. ACM Press, 1991.
2. A. M. Bruckstein. The self-similarity of digital straight lines. In *Proc. 10th Int. Conf. Pattern Recognition (ICPR'1990), Atlantic City, NJ*, volume 1, pages 485–490, 1990.
3. D. Coeurjolly. *Algorithmique et géométrie pour la caractérisation des courbes et des surfaces*. PhD thesis, Université Lyon 2, December 2002.
4. D. Coeurjolly and R. Klette. A comparative evaluation of length estimators of digital curves. *IEEE Transactions on Pattern Analysis and Machine Intelligence*, 26(2):252–258, 2004.
5. F. de Vieilleville. *Analyse des parties linaires des objets discrets et estimateurs de caractristiques gomtriques*. PhD thesis, Université Bordeaux 1, Talence, France, apr 2007.
6. F. de Vieilleville and J.-O. Lachaud. Comparison and improvement of tangent estimators on digital curves. *Pattern Recognition*, 42(8):1693–1707, aug 2009.
7. F. de Vieilleville, J.-O. Lachaud, and F. Feschet. Maximal digital straight segments and convergence of discrete geometric estimators. *Journal of Mathematical Image and Vision*, 27(2):471–502, February 2007.
8. I. Debled-Rennesson and J.-P. Reveillès. A linear algorithm for segmentation of discrete curves. *Int. Journal of Pattern Recognition and Artificial Intelligence*, 9:635–662, 1995.
9. H. Doerksen-Reiter and I. Debled-Rennesson. Convex and concave parts of digital curves. In R. Klette, R. Kozera, L. Noakes, and J. Weickert, editors, *Geometric Properties for Incomplete Data*, volume 31 of *Computational Imaging and Vision*, pages 145–160. Springer, 2006.
10. H.-A. Esbelin and R. Malgouyres. Convergence of binomial-based derivative estimation for c2-noisy discretized curves. In *Proc. Int. Conf. Discrete Geometry for Computer Imagery (DGCI'2009)*, volume 5810 of *LNCS*, pages 57–66. Springer, 2009.
11. F. Feschet. Canonical representations of discrete curves. *Pattern Analysis & Applications*, 8(1):84–94, 2005.

12. F. Feschet and L. Tougne. Optimal time computation of the tangent of a discrete curve: Application to the curvature. In *Proc. Int. Conf. Discrete Geometry for Computer Imagery (DGCI'99)*, volume 1568 of *LNCS*, pages 31–40. Springer Verlag, 1999.
13. A. Gross and L. Latecki. Digitizations preserving topological and differential geometric properties. *Comput. Vis. Image Underst.*, 62(3):370–381, 1995.
14. M. N. Huxley. Exponential sums and lattice points. *Proc. London Math. Soc.*, 60:471–502, 1990.
15. B. Kerautret and J.-O. Lachaud. Multiscale Analysis of Discrete Contours for Unsupervised Noise Detection. In *Proc. Int. Work. on Combinatorial Image Analysis (IWCIA2009)*, volume 5852 of *LNCS*, pages 187–200. Springer, 2009.
16. B. Kerautret and J.-O. Lachaud. Meaningful scales online demonstration. http://kerrecherche.iutsd.uhp-nancy.fr/MeaningfulBoxes, 2010.
17. B. Kerautret and J.-O. Lachaud. Meaningful scales detection along digital contours for unsupervised local noise estimation. *IEEE Transaction on Pattern Analysis and Machine Intelligence*, 2012. Accepted. To appear.
18. R. Klette and A. Rosenfeld. Digital straightness – a review. *Discrete Applied Mathematics*, 139(1-3):197–230, April 2004.
19. Reinhard Klette and Azriel Rosenfeld. *Digital Geometry: Geometric Methods for Digital Picture Analysis*. Morgan Kaufmann Publishers Inc., San Francisco, CA, USA, 2004.
20. J.-O. Lachaud. *Espaces non-euclidiens et analyse d'image : modèles déformables riemanniens et discrets, topologie et géométrie discrète*. Habilitation à diriger des recherches, Université Bordeaux 1, Talence, France, 2006.
21. J.-O. Lachaud and X. Provençal. Two linear-time algorithms for computing the minimum length polygon of a digital contour. *Discrete Applied Mathematics*, 2011. In Press, Corrected Proof, Available online 8 September 2011.
22. J.-O. Lachaud, A. Vialard, and F. de Vieilleville. Fast, accurate and convergent tangent estimation on digital contours. *Image and Vision Computing*, 25(10):1572–1587, 2007.
23. L. J. Latecki, C. Conrad, and A. Gross. Preserving topology by a digitization process. *Journal of Mathematical Imaging and Vision*, 8(2):131–159, mar 1998.
24. X. Provençal and J.-O. Lachaud. Two linear-time algorithms for computing the minimum length polygon of a digital contour. In *Proc. Int. Conf. Discrete Geometry for Computer Imagery (DGCI2009)*, volume 5810 of *LNCS*, pages 104–117. Springer, 2009.
25. J.-P. Reveillès. *Géométrie discrète, calcul en nombres entiers et algorithmique*. Thèse d'etat, Université Louis Pasteur, Strasbourg, France, 1991.
26. Tristan Roussillon and Isabelle Sivignon. Faithful polygonal representation of the convex and concave parts of a digital curve. *Pattern Recognition*, 44(10-11):2693 – 2700, 2011.
27. F. Sloboda, B. Zaťko, and J. Stoer. On approximation of planar one-dimensional continua. In *Advances in Digital and Computational Geometry*, pages 113–160, 1998.
28. A. W. M. Smeulders and L. Dorst. Decomposition of discrete curves into piecewise straight segments in linear time. In R. A. Melter, A. Rosenfeld, and P. Bhattacharya, editors, *Vision geometry: Proc. AMS special session, October 20-21, 1989*, volume 119, pages 169–195, Hoboken, New Jersey, 1991. American Mathematical Society.
29. K. Voss. *Discrete Images, Objects, and Functions in* $\mathbb{Z}^n$. Springer-Verlag, 1993.